Chapter

Stereoscopic Precision of the Large Format Digital Cameras

Benjamin Arias-Perez

Abstract

Stereoscopic vision is fundamental in the task of photogrammetric restitution (stereo compilation) in which, by inserting a floating mark in the 3D observation of pairs of images, it is possible to draw the elements of the terrain in space and obtain cartography of a part of the land cover from aerial images. Initially with film photographs, which were later scanned, and finally with large format digital cameras that began in the 2000s, photogrammetry has undergone a series of technological revolutions up to the present time. In this chapter, after a brief exposition of the basic principles of photogrammetric restitution, a review of current large-format digital cameras and their main implications in restitution is made, which, despite the advances and other similar semi-automatic products (DTM, orthophoto) is still manual and must be operated by a person with the implications that this entails in stereoscopic vision.

Keywords: photogrammetry, aerial digital cameras, stereoscopic precision, Ground Sample Data, photogrammetric restitution

1. Introduction

Photogrammetry (the art and science of determining the position and shape of objects from photographs [1]) has been used since the early 20th century as an efficient method of generating mapping of large areas of the territory, from images obtained with cameras on board an aircraft.

The "General Method of Photogrammetry" describes the stereoscopic processing of images: acquisition of a pair of images that verify artificial stereoscopy conditions; orientation of the images to each other; and virtual three-dimensional exploration of the stereoscopic space generated and cartographic capture of points:

- Acquisition of a pair of images that verify artificial stereoscopy conditions. The process of artificial stereoscopic vision is based on generating an image for the left eye and an image for the right eye (as in natural stereoscopic vision). In photogrammetry, images are separated from each other by a certain distance (called base, b) and the image axes are normal to this base and parallel to each other. This configuration is known as a normal case.

- Orientation of the images to each other. This achieves a stereoscopic model that is also metric (relative to an external reference system).

- Virtual three-dimensional exploration of the stereoscopic space generated and cartographic capture of points. In 1892 Stolze invented the floating mark, which allows metric three-dimensional exploration. Two marks located in photography paths are perceived as a single point located in space. If the observer can move the marks on the images while receiving a stereoscopic perception of them, they can "pose the floating mark" on the surface of the object. This way of obtaining 3D coordinates is known as photogrammetric restitution or stereo compilation (**Figure 1**).

The *XY* precision is directly proportional to the scale of the image, m_b, and the measurement precision of the image, σ_i:

$$\sigma_{xy} = \sigma_i * m_b \tag{1}$$

The precision of the measure on the image plane, σ_i usually ± 6 μm [1] can be expressed in terms of pixel size, *px*, as a fraction (*1/k*). This value k can be considered as an indicator of measurement precision in the image.

$$\sigma_i = \frac{\text{px}}{k} \Rightarrow \sigma_{\text{xy}} = \frac{\text{px}}{k} * m_b \tag{2}$$

Moreover, the product of pixel size for image scale provides the pixel size in the ground, *GSD (Ground Sample Distance)*:

$$\text{GSD} = \text{px} * m_b \Rightarrow \sigma_{\text{xy}} = \frac{\text{GSD}}{k} \tag{3}$$

Thus, the precision observed in *XY* can be expressed as a fraction of the *GSD*. Once the empirical planimetric standard deviation, S_{XY}, is obtained, the empirical measurement precision of the image, S_i is get. From S_i the value of k can be computed which is a good value of comparison between cameras.

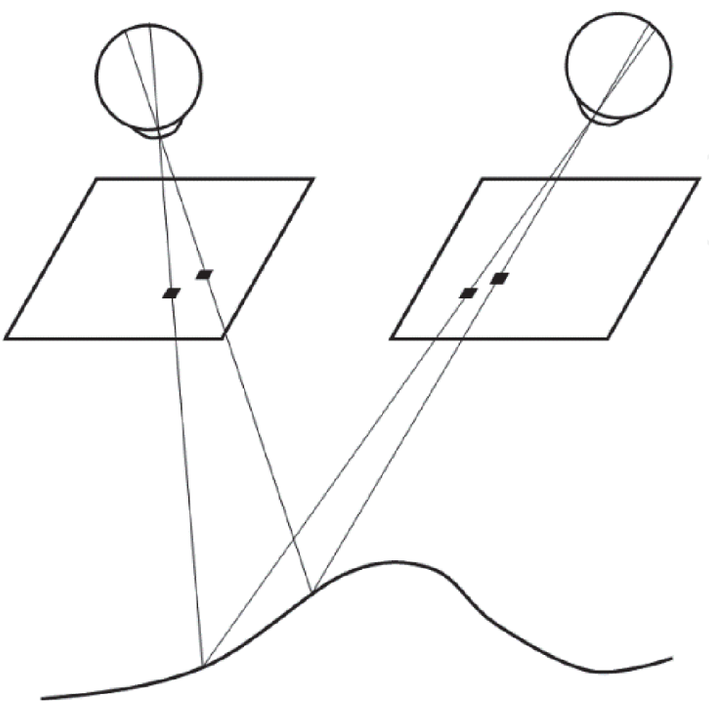

Figure 1.
Floating mark principle.

$$S_{xy} = S_i * m_b \Rightarrow S_i = \frac{S_{xy}}{m_b}$$
$$S_i = \frac{px}{k} \Rightarrow k = \frac{px}{S_i} \tag{4}$$

From this expression it follows that the higher k, the better precision.

It is important to note that σ expresses the theoretical precision while S expresses the empirical standard deviation which is determined from measurements.

The precision in Z, σ_Z, depends on the precision of measurement of the horizontal parallax, σ_{Px}, the image scale, m_b, and the ratio height/base, H/B [1]:

$$\sigma_z = \sigma_{Px} * m_b * \frac{H}{B} \tag{5}$$

The measurement precision of the horizontal parallax can be replaced by the measurement precision in the image plane, σ_i. The ratio height/base can be replaced by the ratio focal/photobase (c/b), then:

$$\sigma_z = \sigma_i * m_b * \frac{c}{b} \tag{6}$$

The precision of the measure in the image plane, σ_i, can be expressed in terms of pixel size as a fraction of it. In this case, it is assigned a value of $1/k$:

$$\sigma_i = \frac{px}{k}$$
$$\sigma_z = \frac{px}{k} * m_b * \frac{c}{b} \tag{7}$$

Moreover, the product of pixel size for image scale provides the pixel size in the ground, *GSD*:

$$GSD = px * m_b$$
$$\sigma_z = \frac{GSD}{k} * \frac{c}{b} \tag{8}$$

As can be seen, precision in Z can also be expressed in terms of the *GSD*, the focal length and photobase. This is a function of longitudinal overlap, R_L, together with the image width:

$$b = (1 - R_L) * \text{width} \tag{9}$$

Camera	c (mm)	Width (mm)	b (R_L = 60%) (mm)	c/b
Analogue	150	220	88	1,70
DMC	120	95	38	3,16
UltraCamD	100	67,5	27	3,70
DMC III	92	56,9	22.8	4,04
UltraCam Eagle M3 f80	80	68	2722	2,94
UltraCam Eagle M3 f210	210	68	27.2	7,72

Table 1.
Ratios c/b *or various photogrammetric aerial cameras, calculated for a longitudinal overlap of 60%.*

The value *c/b* affects proportionally the *Z* precision, so that the higher the value of this ratio less precision in *Z* (**Table 1**).

2. Aerial digital cameras

2.1 Technological evolution: film to digital

Photogrammetry has undergone three digital revolutions. The first took place in the 1980s with the digitization of the mathematical model that resulted in analytical stereoplotters (process input, frames, remained analogue). Analogue stereoplotters that solved the mathematical model by mechanical analogy disappeared.

The second occurred in the 1990s with digitization, using powerful and accurate photogrammetric scanners, analogue images from the aircraft that resulted in digital stations. This revolution was possible when personal computers had sufficient capacity to efficiently handle digital images, and represented the extinction of analytical stereoplotters and, with them, the stereoplotters themselves; that is, of the specific physical machines used for photogrammetry.

The third revolution took place in the first decade of the 21st century thanks to the development of digital cameras that began to compete with the large format (230 x 230 mm) of analogue cameras. These cameras were already used in terrestrial photogrammetry, where the small and medium formats were enough to develop projects. The need to cover large areas of land in aerial photogrammetry made the large size of the camera the only possible solution between the two photogrammetric requirements: accuracy (requiring long focal length), and performance in object coverage (requiring either short focal or large focal planes). This phase involves the disappearance of analogue cameras and, consequently, films. Therefore it will also represent the disappearance of photogrammetric scanners (**Table 2**).

The main advantages of digital versus analogue images are [2]: the ability to establish an entirely digital workflow (suppressing the scanners), a considerable improvement in radiometric quality as well as the possibility of simultaneously acquiring panchromatic images in the different color bands and in the near infrared; as well as the ability to generate real-time mapping [3]. The color depth of digital cameras (12-bit) should allow flights to be carried out in poor lighting conditions [4].

A first approach to digital cameras for photogrammetric use allows them to be classified into two large groups: frame and pushbroom. The first can be classified according to the size of the sensor [5]: small format cameras (up to 16 megapixels); medium format cameras (from 16 to 50 megapixels); and large format cameras (50 megapixels or higher). More recently, medium format can be located at 80–100 megapixels [6], and large format larger than 100 megapixels.

	It consists of	**Appears**	**Disappears**
First revolution (80s)	Digitizing the mathematical model	Analytical stereoplotters	Analogue stereoplotters
Second revolution (90s)	Post-flight scanning of the image	Digital station Photogrammetric scanner	Analytical stereoplotters
Third revolution (00s)	In-flight scanning of the image	Digital aerial camera	Analogue aerial camera Aerial films Photogrammetric scanner

Table 2.
Evolution of digital photogrammetry.

2.2 Cameras in the photogrammetric mapping sector

The two large manufacturers of analogue cameras for aerial photogrammetry took the first steps towards digital cameras around 2000, each opting for a different technology. Leica, who manufactured the RC30 model, used a pushroom camera, ADS40, based on space sensors (HSRC, WAAC) from the German institute DLR. Meanwhile, Z/I Imaging moved from the RMK-TOP analogue model to the DMC modular camera in 2000 (synchronous mode).

Following the launch in 2000 of ADS40 and DMC, Vexcel, manufacturer of scanners for photogrammetric use, offered the UltraCamD digital camera to the market in 2003 (syntopic mode).

Currently there are also other large format cameras and even some medium format ones competing for the same sector, but it is not our intention in this chapter to give a review of the current offer of cameras for mapping, only to study the characteristics related to stereoscopic accuracy. To do this, the current models of Leica, Z/I Imaging (now both in Hexagon Group) and Vexcel are considered representative: DMC III and UltraCam Eagle M3. In addition, they allow working with interchangeable lenses, which adds versatility so as to be able to use the most appropriate focal length for each use: short for mapping purposes, and long for orthophotos generation.

The sensors of large format digital cameras are clearly smaller in size than conventional cameras (Width in **Table 3**). To find an easily interpretable equivalence, we could say that, in order for digital cameras to compete with analogue, it must be assumed that there is an equivalence between 20 μm, the size of the scanned pixel, and the 10 μm average pixel size in a digital camera (**Table 3**).

Initially, the equivalence between 20 μm scanned and 10 μm digital is assumed by the manufacturers of these cameras because they think that the digital pixel is of higher quality than the scanned pixel [7]. According to these same authors, different experiments indicate that automatic matching is 2,5 times better in the case of a digital image.

Angular resolution refers to the angle subtended by a pixel from the point of view. The initial digital cameras can be considered equivalent to the 15 μm scan; however, the current ones are much better (less than 10″).

Figure 2 provides a comparison of a reticle photographed and scanned at a resolution of 5, 10 and 15 μm (a, b and c) while on the right (d) the same grid obtained directly by a digital camera appears.

Camera	Width (mm)	Pixel size (μm)	Focal lenght (mm)	Angular resolution (″)	AGL (m) for GSD = 0,10 m
Analogue	220	20	150	28	750
Analogue	220	15	150	21	1000
DMC	168	12	120	21	1000
UltraCamD	103,5	9	100	19	1111
DMC III	56,9	3,9	92	9	2359
UltraCam Eagle M3 f80	68	4	80	10	2000
UltraCam Eagle M3 f210	68	4	210	4	5250

Table 3.
Data of large format digital cameras.

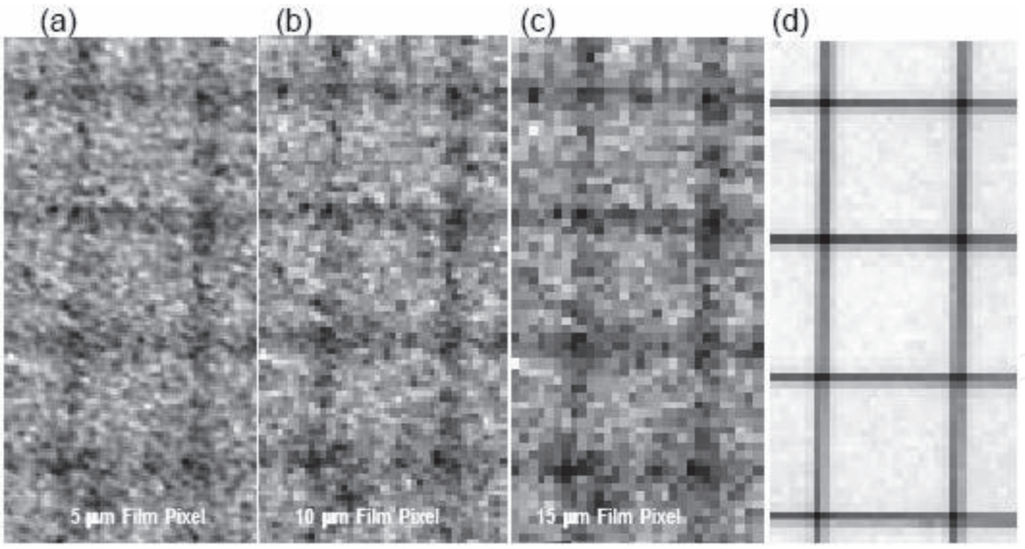

Figure 2.
A reticle photographed and scanned at a resolution of 5, 10 and 15 µm (a, b and c). The same grid obtained directly by a digital camera (d) [8].

3. Stereoscopic performance

Another issue in favor of digital cameras is their increased ability to get more images [7]. This gives them an advantage in terms of the possibility of achieving greater redundancy in the aerotriangulation process, and obtaining greater overlaps that decrease the overlap in the direction of flight.

The following sections provide a theoretical analysis of the stereoscopic performance of the DMC and UltraCam compared to the performance of analogue cameras.

3.1 Frame rate

Considering an airplane speed of 75 m/s and a *frame rate* of 1 second, the movement of the aircraft between two shots is 75 metros. The image size, in the case of the UltracamD camera, is 7.500 pixels in the direction of flight (*along track*). If the longitudinal overlap is 60%, this means that the base is 3.000 pixels. In this way, the minimum GSD with stereoscopic overlap that can be obtained with 60% longitudinal overlap is 25 mm.

$$\mathrm{GSD}_{\mathrm{minimum}} = \frac{\mathrm{Desplaz}}{\mathrm{Px} * (1 - R_L)} \tag{10}$$

Where *Desplaz* is the displacement of the aircraft between two shots (75 m), *Px is* the number of pixels of the sensor in the direction of flight (7.500), R_L is the longitudinal overlap (60%).

This means that images with GSD from 25 mm to 90% cannot be achieved, because the plane cannot fly that slowly (750 pixels * 25 mm = 18,75 m). These 25 mm imply a flight height 277,78 m:

$$H = \frac{c}{\mathrm{sx}} * \mathrm{GSD} \tag{11}$$

where f is the focal length (100 mm), sx the pixel size (9 µm) and GSD is Ground Sample Distance (25 mm).

The following **Tables 4–6** show the resulting minimum *stereoscopic* GSD sizes for different longitudinal overlaps, for *UltraCamD, UltraCamX,* and *DMC cameras*.

RL (%)	GSD min (m)	H (m)
60	0,025	277,778
70	0,033	366,667
80	0,050	555,56
90	0,10	1111,111

It has been considered an aircraft speed of 75 m/s and a frame rate of 1 second (base on the ground of 75 meters).

Table 4.
Minimum stereoscopic GSD sizes and their corresponding flight height (H) for the UltraCamD camera (Px = 7.500; sx = 9 μm; f = 100 mm), given the desired longitudinal overlap (RL).

RL (%)	GSD min (m)	H (m)
60	0,020	276,451
70	0,027	368,601
80	0,040	552,902
90	0,080	1105,803

It has been considered an aircraft speed of 75 m/s and a frame rate of 1 second (base on the ground of 75 meters).

Table 5.
Minimum stereoscopic GSD sizes and their corresponding flight height (H) for the UltraCamX camera (P = 9.420; sx = 7.2 μm; f = 100 mm), given the desired longitudinal overlap (R_L).

RL (%)	GSD min (m)	H (m)
60	0,049	488,281
70	0,065	651,042
80	0,098	976,563
90	0,195	1953,125

It has been considered an aircraft speed of 75 m/s and a frame rate of 1 second (base on the ground of 75 meters).

Table 6.
Minimum stereoscopic GSD sizes and their corresponding flight height (H) for the DMC camera (P = 7.680; sx = 12 μm; f = 120 mm), given the desired longitudinal overlap (RL).

3.2 Coverage

A fundamental part of any photogrammetric flight project is determining the direction and number of passes, number of total and past photographs, among other data. All this is determined from a series of initial conditions that establish the work area, which define the scale of the photograph to be obtained, etc...

First, a flight made with analogue camera is analyzed, for example, with the following characteristics:

- Scale of photography: 1:20.000
- Scanning photo size: 15 μm.
- Useful photo size: 220x220 mm.

This provides a GSD of:

$$15\mu m * 20.000 = 300 \text{ mm} \tag{12}$$

considering that each frame has a useful format of 220x220 mm, due to the space reserved in the frame for marginal information, the surface contained per frame is:

$$\begin{aligned} &220 \text{ mm} * 20.000 = 4.400 \text{ m} \\ &4.400 * 4.400 = 1.936 \text{ Ha} \end{aligned} \tag{13}$$

Now, with that same GSD, the resulting area for the *UltraCamD image* is:

$$\begin{aligned} &11.500 \text{ pixels} * 300 \text{ mm} = 3.450 \text{ m} \\ &7.500 \text{ pixels} * 300 \text{ mm} = 2.250 \text{ m} \\ &3.450 * 2.250 = 776,25 \text{ Ha} \end{aligned} \tag{14}$$

Comparing both surfaces,

$$\frac{1.936}{776,25} = 2,49 \tag{15}$$

This means that approximately the 2.5-frame area of *UltraCamD is required* to cover the same surface as an analogue image. However, in the particular case of a frame, this is not true due to the different shapes of these (analog and rectangular square in digital camera). However, if the approach is generic, i.e., to cover a certain area for a project, that relationship can actually be valid.

3.3 Number of frames

Considering first longitudinally, and with the overlap of 60%, each new frame adds one side of 40% more to the strip. That is, the covered length, *L,* by *n* frames of a certain width, is determined by:

$$\begin{aligned} &L = \text{width} * \text{n} * 40\% \\ &L = \text{width} * \text{n} * (100 - R_L) \end{aligned} \tag{16}$$

To relate the number of photos to both flights to cover the same *length L*, with the same longitudinal overlap, this ratio is determined by the relationship between the widths of the frames, calculated above (Eqs (13) and (14)):

$$\frac{4.400}{2.250} = 1,956 \tag{17}$$

Similar reasoning can be followed for cross-sectional overlap:

$$L = \text{high} * \text{n} * (100 - R_T) \tag{18}$$

which in the example provides the following relationship:

$$\frac{4.400}{3.450} = 1,275 \tag{19}$$

If we now want to know the relationship between the total number of photographs between the two flights:

Camera	Useful width	Useful height	Coverage	Ratio
Analogue	220 mm	220 mm	1.936 Ha	—
UltraCamD	7.500 pixels	11.500 pixels	776,25 Ha	2,49
UltraCamX	9.420 pixels	14.430 pixels	1.223,38 Ha	1,58
DMC	7.680 pixels	13.824 pixels	955,51 Ha	2,03

Table 7.
Surfaces contained in a frame for different cameras, considering in all cases a GSD, where ratio expresses the ratio between the coverage of the analog camera and the coverage of the digital camera 300 mm.

$$1,956 * 1,275 = 2,49 \tag{20}$$

corresponding to the amount found in Eq. (15).

3.4 Conclusions on coverage

The relationship between the number of frames taken with analog camera and *UltraCamD* digital camera depends on the size of the pixel in the field, GSD. That is, by imposing a certain size of GSD, the relationship between the number of frames in both cameras is determined at the same time.

With the digital camera it is enough to multiply the number of pixels in height and width of the image by the GSD to obtain the actual magnitudes of the terrain to be covered with each frame In addition, it is clear that said GSD, the pixel size in the CCD, and the focal length will determine the flight height and scale of the photograph (**Table 7**).

While with the analog camera it is necessary to determine either the frame scale or the scanning pixel (variable depending on the scanner). Depending on one parameter, the other parameter is obtained. However, it is true that it is scanned at 15–20 μm., therefore, usually this pixel size determines the frame scale.

Acknowledgements

Department of Cartographic and Land Engineering, University of Salamanca.

Author details

Benjamin Arias-Perez
Department of Cartographic and Land Engineering, University of Salamanca, Ávila, Spain

*Address all correspondence to: benja@usal.es

References

[1] KRAUS, Karl; WALDHÄUSL, P. Photogrammetry Fundamentals and Standard Processes. vol. 1. Dümmler, Bonn,, 1993, vol. 14.

[2] Heipke, C., Jacobsen, K., Mills, J. Editorial Theme issue: "Digital aerial cameras". ISPRS Journal of Photogrammetry and Remote Sensing. 2006;60.6:361–362. DOI: 10.1016/j.isprsjprs.2006.06.004

[3] Tempelmann, U., Börner, A., Chaplin, B., Hinsken, L., Mykhalevych, B., Miller, S., Recke, U., Reulke, R., Uebbing, R. Photogrammetric Software for the LH Systems Airborne Digital Sensor. International Archives of Photogrammetry, Remote Sensing and Spatial Information Sciences. 2000;33. B2:552–559.

[4] Markelin, L.,Ahokas, E., Honkavaara, E., Kukko, A. Peltoniemi, J. Radiometric quality comparison of UltraCamD and analog camera. International Archives of Photogrammetry, Remote Sensing and Spatial Information Sciences. 2005;34.

[5] Petrie, G. Further Advances in Airborne Digital Imaging - Several New Imagers Introduced at ASPRS. GeoInformatic. 2006;9.8:16–23.

[6] RAIZMAN, Yuri. Productivity Analysis for Medium Format Mapping Cameras. Photogrammetric Engineering & Remote Sending. 2018;84.5:235–238.

[7] Leberl, F., Gruber, M., Ponticelli, M., Bernoegger, S., & Perko, R. The UltraCam large format aerial digital camera system. Proceedings of the American Society For Photogrammetry & Remote Sensing. 2003;sn:5–9.

[8] Perko, Roland; Gruber, Michael. Comparison of quality and information content of digital and film-based images. International Archives of Photogrammetry, Remote Sensing and Spatial Information Sciences. 2002;34.3/B:206–209.